Polymer

Volume 103, 26 October 2016, Pages 9–18

http://dx.doi.org/10.1016/j.polymer.2016.09.031

http://www.sciencedirect.com/science/article/pii/S003238611630831X

INTERACTIONS, STRUCTURE AND PROPERTIES IN PLA/PLASTICIZED STARCH BLENDS

P. Müller[1,2], J. Bere[1,2], E. Fekete[1,2], J. Móczó[1,2,*], B. Nagy[1,3], M. Kállay[1,3], B. Gyarmati[1], and B. Pukánszky[1,2]

[1]Department of Physical Chemistry and Materials Science, Budapest University of Technology and Economics, H-1521 Budapest, P.O. Box 91, Hungary

[2]Institute of Materials and Environmental Chemistry, Research Centre for Natural Sciences, Hungarian Academy of Sciences, H-1519 Budapest, P.O. Box 286, Hungary

[3]MTA-BME Lendület Quantum Chemistry Research Group

*Corresponding author: Phone: +36-1-463-3477, Fax: +36-1-463-3474, Email: jmoczo@mail.bme.hu

Abstract

Blends were prepared from poly(lactic acid) (PLA) and thermoplastic starch (TPS) to study component interactions, structure and properties. Starch was plasticized with glycerol at two levels, at 36 and 47 wt%. The results unambiguously showed that the interaction of the two components is weak. The investigation of the possible partitioning of glycerol in the two phases indicated that most of the plasticizer is located in the TPS phase. Thermodynamic modeling predicted some dissolution of PLA in TPS which was assisted by the presence of the plasticizer, but TPS did not dissolve in PLA at all. No tangible proof was found for the formation of a glycerol rich phase in TPS, the relaxation transition assigned to this phase was rather explained with the movement of smaller structural units of starch molecules. Weak interfacial adhesion does not allow stress transfer through the interface resulting in poor strength and small deformation.

Keywords: thermoplastic starch, molecular modeling, thermodynamics,

1. Introduction

In recent years the importance of biopolymers increases continuously and further growth is forecasted in their use in the future. However, besides the obvious environmental advantages of these materials, they have some deficiencies as well, like inferior properties compared to commodity polymers, poor processability, water sensitivity, etc. To overcome these drawbacks biopolymers are frequently modified, often by blending. The mixing of poly(lactic acid) (PLA) and thermoplastic starch would combine the advantages of the two polymers by maintaining complete biodegradability and resulting in a relatively cheap material [1-5]. However, the two polymers are immiscible, heterogeneous blends form upon their mixing, and the statements about the compatibility of TPS and aliphatic

polyesters are often contradictory. Avérous and Fringant [6, 7] found dissimilar compatibility in various starch/aliphatic polyester blends. In a further study Martin and Avérous [8] claimed low level of compatibility in PLA/TPS blends, but in another part of the same paper they state that changes in T_g indicate some interaction between TPS and PLA. The degree of compatibility claimed varies in a wide range depending on blend components and the authors of the paper. Ma et al. [9, 10], for example, found complete immiscibility in PLA/TPS blends when the plasticizer was glycerol, while good compatibility, when formamide was used. However, the statements on compatibility or miscibility are almost invariably qualitative in nature and based on the observation of SEM micrographs, changes in T_g or mechanical properties, but rarely on thermodynamic considerations. Poor compatibility of the components is also indicated by attempts to improve interactions by preparing hybrid blends[11] , adding amphiphilic molecules [12] or a coupling agent [13].

Another interesting question that is never discussed or even mentioned in relation with TPS blends is the role of the plasticizer. Although many papers have been published on TPS plasticized with the most diverse compounds, on their efficiency and on the structure formed, TPS is treated as a single, homogeneous material in blends, in spite of the fact that TPS plasticized with glycerol was claimed to phase separate above a certain plasticizer content [6, 7, 14-17]. The distribution of a third material, e.g. the aliphatic polyester, in a two phase polymer, TPS, can be quite complicated, several structures may form and must be considered. Moreover, the plasticizer is a small molecular weight substance which is quite mobile at the temperature of processing, but also under ambient conditions. Although originally it is located in starch, it may diffuse into the other polymer during processing and partition between the two polymer components. Although Ma et al. [9, 10] claimed improvement in compatibility upon the use of formamide compared to

glycerol, they did not explain the effect or its mechanism either. In view of these questions, the goal of this work was to estimate interactions in PLA/TPS blends by thermomechanical analysis [18-20] and thermodynamic modeling, study the role and partitioning of the glycerol plasticizer in the components and determine the structure and properties of the blends in a wide composition range.

2. Experimental

2.1. Materials

The PLA used was obtained from NatureWorks (USA). The selected grade (Ingeo 4032D, M_n = 88500 g mol^{-1} and M_w/M_n = 1.8) is recommended for extrusion. The polymer (<2 % D isomer) has a density of 1.24 g cm^{-3}, while its melt flow index (MFI) is 3.9 g/10 min at 190 °C and 2.16 kg load. The corn starch used for the preparation of TPS was supplied by Hungrana Ltd., Hungary and its water content was 12 wt%. Glycerol with 0.5 wt% water content was obtained from Molar Chemicals Ltd., Hungary and it was used for the plasticization of starch without further purification or drying. Thermoplastic starch samples containing 36 and 47 wt% glycerol (TPS36 and TPS47, respectively) were prepared and used in the experiments. The composition of the PLA/TPS blends changed from 0 to 1 volume fraction in 0.1 volume fraction steps. Glycerol was added to PLA also alone as "plasticizer" in 1, 3, 5, 7 and 10 vol%.

2.2. Sample preparation

Corn starch was dried in an oven before composite preparation (105 °C, 24 hours). Thermoplastic starch powder was prepared by dry-blending in a Henschel FM/A10 high speed mixer at 2000 rpm. TPS was produced by processing the dry-blend on a Rheomex 3/4" single screw extruder attached to a Haake Rheocord EU 10 V driving unit at 140-150-

160 °C barrel and 170 °C die temperatures, and 60 rpm screw speed.

PLA and the second component were homogenized in an internal mixer (Brabender W 50 EHT) at 190 °C and 50 rpm for 12 min. Before homogenization poly(lactic acid) was dried in a vacuum oven (110°C, 4 hours). Both temperature and torque were recorded during homogenization. The melt was transferred to a Fontijne SRA 100 compression molding machine (190 °C, 5 min) to produce 1 mm thick plates for further testing.

2.3. Characterization

The glass transition temperature of the phases and other thermal transitions appearing in the blends were determined by dynamic mechanical analysis (DMA) using a Perkin Elmer Pyris Diamond DMA apparatus in tensile mode with constant amplitude (10 μm) and frequency (1 Hz) in the temperature range between -100 and 100 °C. Heating rate was 2 °C/min, while the size of the specimens was 50 x 5 x 1 mm. Mechanical properties were further characterized by tensile testing using an Instron 5566 universal testing machine. Specimens of 150 x 10 x 1 mm were used, the gauge length was 115 mm. Tensile modulus was determined at 0.5 mm/min, while properties measured at larger deformations at 5 mm/min cross-head speed. Five parallel measurements were carried out at each blend composition. The structure of the blends was analyzed by scanning electron microscopy (SEM) using a Jeol JSM 6380 LA apparatus. Samples were broken at liquid nitrogen temperature and then a smooth surface was created by cutting the sample with a microtome. Surfaces were etched according to the matrix polymer, chloroform was used in the case of PLA, while 1 M HCl for the TPS matrix. Light transmittance through the samples was measured on 1 mm thick specimens using a Unicam UV-500 spectrophotometer at 700 nm wavelength. Water absorption was determined at 23 °C and 52 % relative humidity by the measurement of the weight increase of specimens. The

desired relative humidity was achieved with a saturated solution of $Mg(NO_3)_2$.

3. Results and discussion

The results are presented in several sections. The question of component interaction and miscibility is discussed first and then the effect of the plasticizer on PLA properties is presented subsequently. Conclusions drawn from these results are supported by model calculations in the next section followed by the discussion of structure and properties.

3.1. Interactions, miscibility

One of the most often used approaches to estimate the miscibility of two components is the determination of the composition dependence of the glass transition temperature of their blends [18-20]. The DMA spectra of a PLA/TPS47 blend containing 50 vol% of both components is presented in **Fig. 1**.

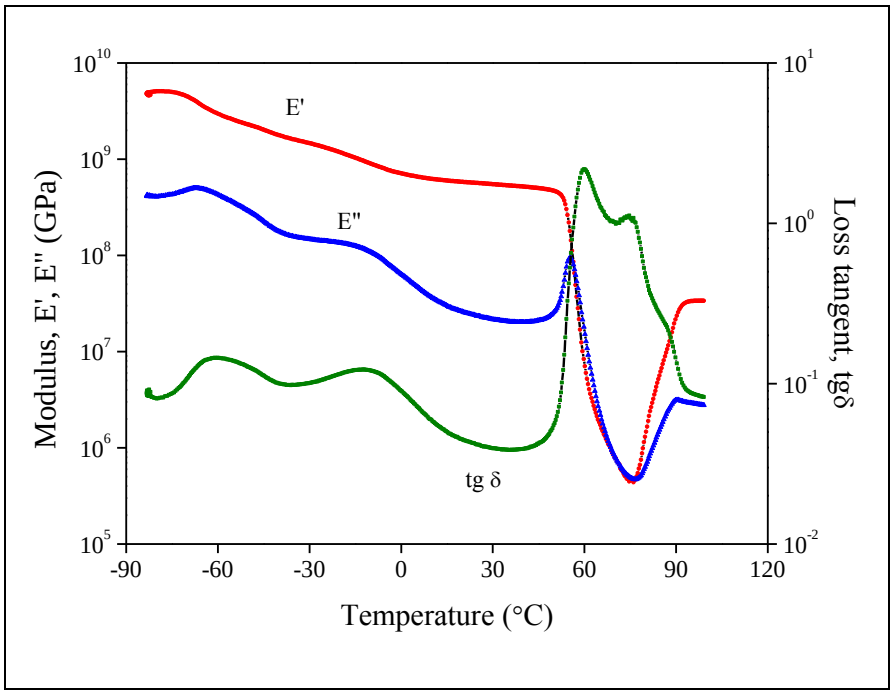

Fig. 1 DMA spectra showing relaxation transitions in the PLA/TPS47 blend containing 50 vol% of both components.

The spectra are rather complicated displaying several transitions. Plasticized starch were shown to exhibit two transitions, one corresponding to its glass transition, while the second was claimed to result from phase separation and was assigned to a glycerol rich phase [6, 7, 14-17]. The glass transition temperature of TPS depends very strongly on the type and amount of the plasticizer used and it may cover a wide range of temperatures from -30 to 90 °C. The T_g of our TPS samples are -3 and 33 °C for TPS47 and TPS36, respectively. The second transition assigned to thermoplastic starch can be also identified in the spectra allegedly indicating the presence of a glycerol rich phase [6, 7, 14-17]. However, some doubts may arise about the assignment of this transition. Some authors argue that the appearance of two peaks proves phase separation a priori [15] that is not true; several polymers are known to show β relaxation peaks without the presence of a second component (e.g. PMMA, PVC). Phase separation was mentioned only as a possibility anyway in the much cited paper of Kalichevsky [14], but later it was treated as fact [6, 7]. Basically none of the papers mentioning phase separation show any other evidence, but reference to earlier papers and the appearance of two peaks in DMA spectra. Occasionally, the claim might be supported by the analysis of the composition dependence of T_g or the activation energy of the transition, but no direct evidence. The relaxation transition in question appears around -50 or -60 °C that is claimed to be close to the T_g of glycerol at -78 °C and used as a strong argument for the formation of a glycerol rich phase. Phase separation was said to occur above 27 wt% glycerol content. Unfortunately, a number of facts contradict or at least question the hypothesis of phase separation. First of all we do not believe that -50 °C is close to -78 °C. The β peak appeared also at 15 wt% glycerol content in the work of Mikus et al. [17] below the claimed composition of phase separation.

Moreover, the transition was detected at around 0 and -10 °C in TPS plasticized with sorbitol and mannose, respectively, as shown by the same paper [17]. Finally, similar β transition was observed in grafted cellulose acetate and benzylated wood which do not contain any external plasticizer [21, 22]. Accordingly, we think that the transition belongs to smaller units of the amylopectin chain, like a single glucose ring, the movement of which becomes possible upon plasticization. The position of the peak depends on the type and amount of the plasticizer which forms strong secondary interactions with starch molecules. However, the possible phase separation of the glycerol might be important for the phase structure and properties of TPS blends and cannot be ignored. The limited miscibility of starch and glycerol is shown by the exudation of the plasticizer at large glycerol contents, and Stading et al. [23] showed heterogeneous structure in their plasticized starch films.

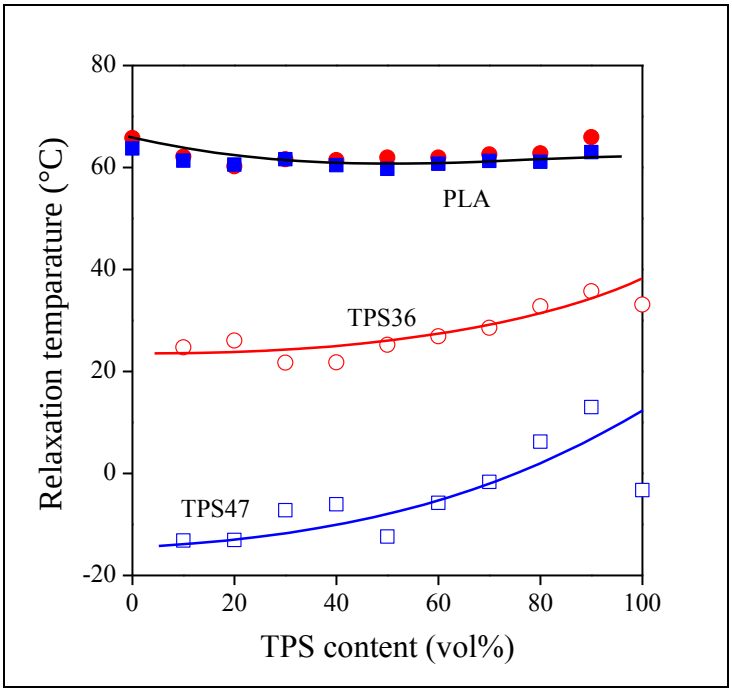

Fig. 2 Effect of composition on the glass transition temperature of the components in PLA/TPS blends; (○,●) TPS36, (□,■) TPS47; full: PLA, empty: TPS.

The remaining two transitions observed in the spectra of the PLA/TPS blend shown in **Fig. 1** can be assigned to PLA. The glass transition of the polymer results in a sharp peak on the tan δ trace and the cold crystallization of the polymer leads to another, smaller transition as well. Accordingly, the glass transition temperatures of the two polymers can be identified unambiguously. Conclusions about miscibility are often drawn from the composition dependence of the glass transition temperature of the blend or its components [18-20]. The T_g of the two blend series is plotted against composition in **Fig. 2**. Separate transition temperatures can be identified for the two polymers. The T_g of PLA is detected at around 65 °C, it does not seem to depend on the amount of plasticizer in TPS and decreases slightly with increasing TPS content. Similar changes were observed by others and led them to the conclusion of partial miscibility [8]. However, the T_g of PLA was shown to decrease also in the presence of particulate fillers [24, 25] and we cannot claim partial miscibility in that case. Moreover, if the components are partially miscible, the T_g of TPS should increase, instead of decreasing, with increasing PLA content. Changes in T_g opposite to the direction expected have been observed earlier for various combinations of polymers. The phenomenon occurs relatively often in impact modified polymers, in which the T_g of the elastomeric phase decreases with increasing concentration of the stiffer component [26-29]. The decrease was explained with the development of negative hydrostatic pressure during cooling resulting from the different thermal expansion coefficients of the components [27]. The condition for the decrease of T_g is the good adhesion of the phases resulting in volume dilatation and increased free volume. The opposite effect was observed in polystyrene (PS)/polypropylene (PP) blends, in which the T_g of PS increased with increasing PP content [30]. The effect was explained again with the difference in thermal expansion coefficients and shrinkage during the crystallization of PP leading to positive hydrostatic pressure this time. In our case, however, the explanation

is more difficult, since the T_g of the TPS phase decreases which would require the good adhesion of the phases. This is not probable thus the reason for the decrease remains unclear and needs further study and considerations. Obviously, a more detailed investigation of thermal expansion coefficients, the developing stress fields and interfacial adhesion must be carried out in the future in order to reveal the actual reason for the change in the glass transition temperature of the TPS phase. Accordingly, the only conclusion that we can draw from the analysis of DMA spectra and the composition dependence of the T_g of the components is that they are immiscible with each other and even partial miscibility must be very small.

Other measurements may supply further, indirect evidence about the miscibility or immiscibility of the components. The light transmittance of the blends is plotted against composition in **Fig. 3**.

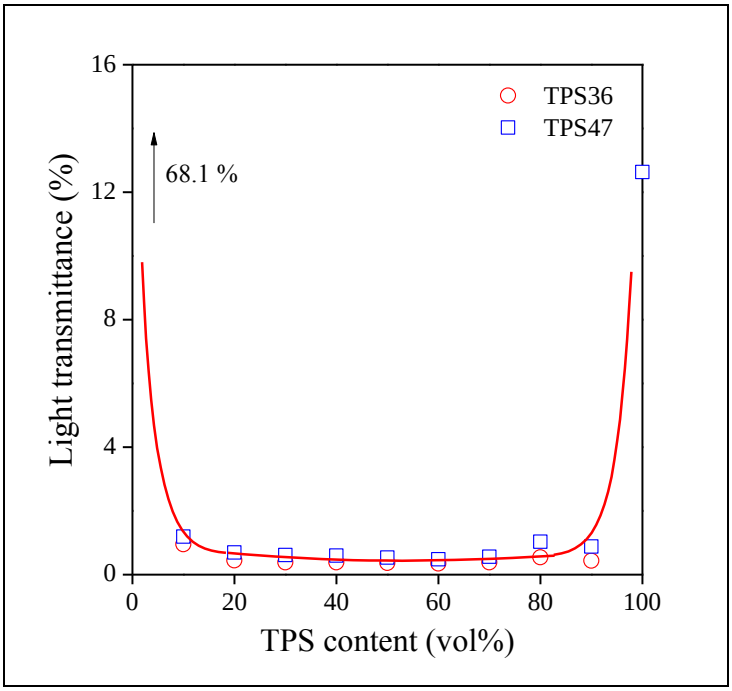

Fig. 3 Effect of blend composition on the light transmittance of PLA/TPS blends; (○) TPS36, (□) TPS47.

PLA is transparent, 68 % of the incident light passes through it. Light transmittance of TPS is smaller, 14.7 and 20.2 % for TPS47 and TPS36, respectively, indicating a slightly heterogeneous structure. However, the transparency of the PLA/TPS blends is extremely small, it is below 1 % at most compositions indicating very poor miscibility and a heterogeneous structure. Obviously, interactions between the two blend components cannot be very strong and phase separation occurs at all compositions. Another indication for poor interactions is supplied by the results of water absorption measurements (**Fig. 4**).

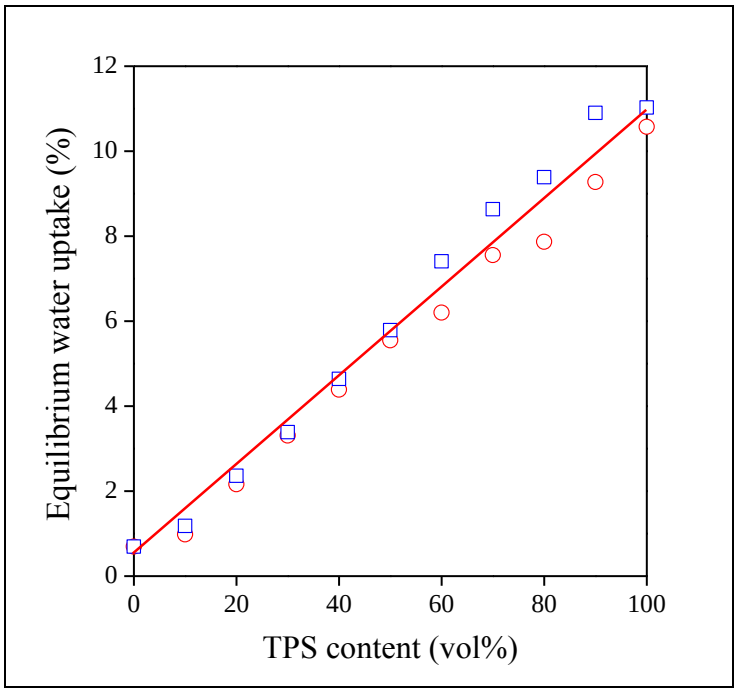

Fig. 4 Independence of the water absorption of PLA/TPS blends of blend composition and glycerol content; (○) TPS36, (□) TPS47.

If the interaction between two polymer components is strong, water or any other solvent must compete for active sites and absorption will be smaller than that dictated by additivity. As **Fig. 4** shows, water absorption in PLA/TPS blends follows almost perfectly additivity indicating the weak interaction of the components.

3.2. PLA/glycerol interaction

Similarly to others we treated TPS as a single, homogeneous material up to now. However, to check the possible effect of glycerol diffusion into PLA, measurements were done on PLA modified with different amounts of glycerol. The transmittance of light through 1 mm thick PLA plates containing various amounts of the plasticizer is plotted against composition in **Fig. 5**.

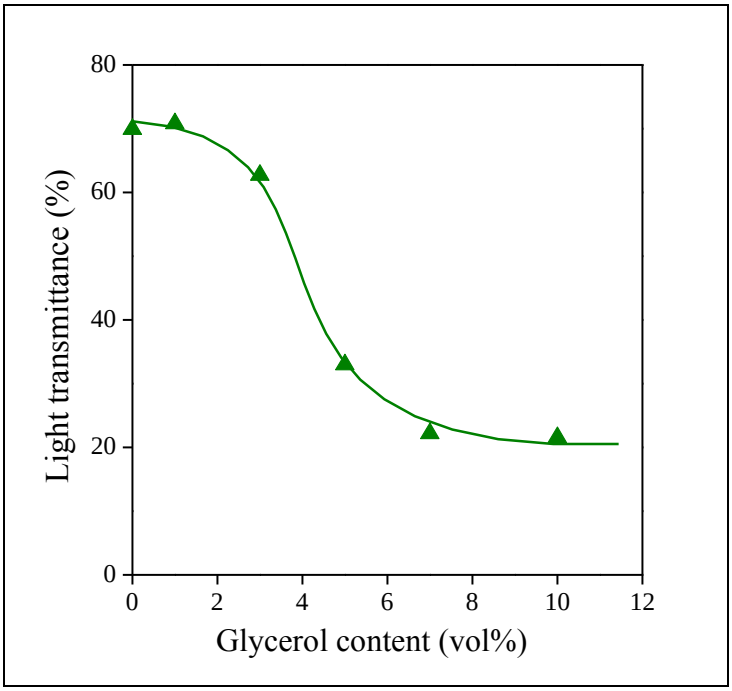

Fig. 5 Effect of glycerol content on the light transmittance of PLA/glycerol binary blends.

PLA is transparent, as mentioned above, but transparency decreases considerably with increasing glycerol content. According to the correlation the solubility of glycerol cannot be more than 1 or 2 vol% in PLA, above this amount a separate phase forms. Dispersed glycerol droplets scatter light resulting in inferior transparency. Obviously, the solubility of glycerol in PLA is quite small, thus one cannot expect considerable diffusion of the plasticizer from starch into the PLA phase in the blends.

Limited solubility of glycerol in PLA is further confirmed by the results of DMA

measurements. The spectra recorded on PLA containing 10 vol% glycerol is presented in **Fig. 6**.

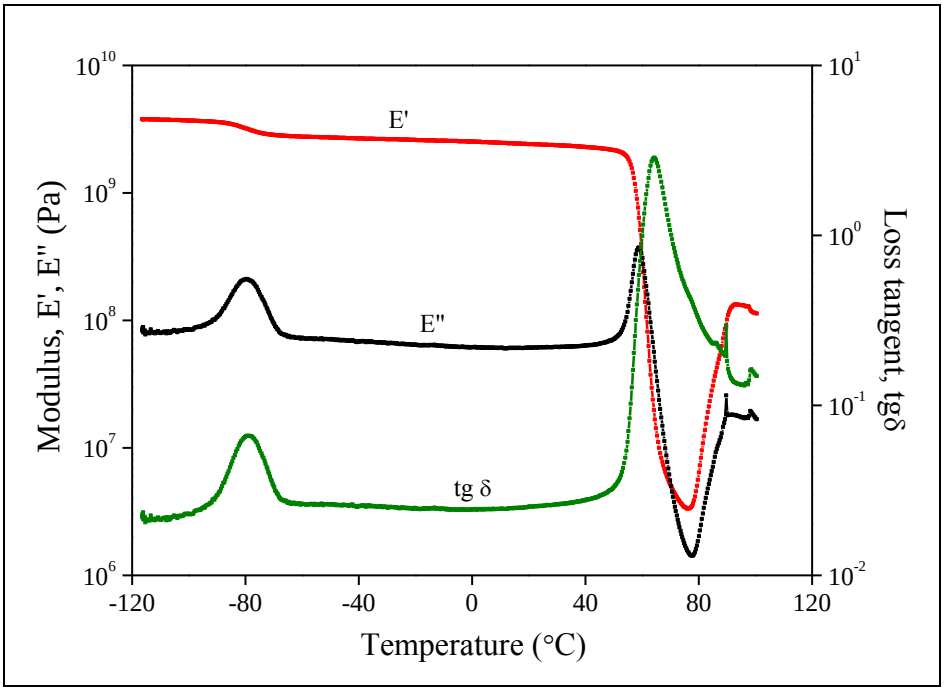

Fig. 6 DMA spectra of the PLA/glycerol binary blend containing 10 vol% of the plasticizer. Strong glycerol transition at low temperature.

The spectra show the typical behavior of PLA, glass transition around 65 °C and the subsequent cold crystallization of the polymer. However, an additional transition also appears on the spectra at very low temperatures, around -80 °C. The transition can be assigned to glycerol and its temperature corresponds to that determined for this plasticizer by Avérous et al. [6] using DSC. The nearly linear increase of the intensity of the tg δ peak with increasing amount of glycerol in the blend, at least at small glycerol contents, further confirms the assignation (**Fig. 7**). The deviation from the expected linearity at the largest glycerol content might result from changing morphology or simply from experimental error. However, since the transition can be detected already at the smallest glycerol content, below 1 vol%, we must assume that the solubility of glycerol in the blend is smaller even

than this amount, since dissolved glycerol would shift the glass transition temperature of PLA and would not appear as a separate peak on the tg δ vs. temperature trace. The study of PLA/glycerol blends confirmed our previous conclusions and indicated that the interaction between PLA and the plasticizer is relatively weak resulting in very limited solubility.

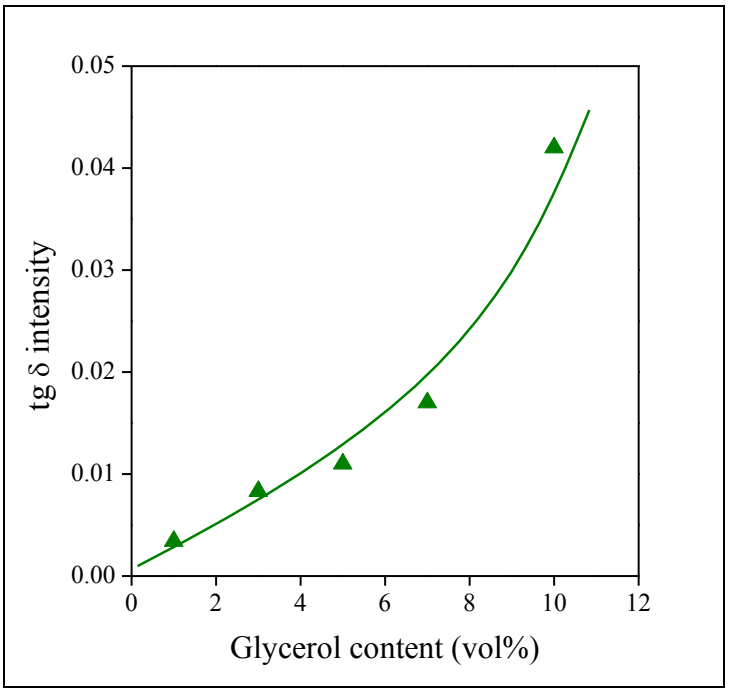

Fig. 7 Influence of composition on the intensity of the tg δ peak assigned to the glass transition of glycerol.

3.3. Modeling

Density functional theory (DFT) and local coupled-cluster calculations with single, double and perturbative triple excitations [LCCSD(T)] have been performed to investigate hydrogen bond interactions between poly(lactid acid) and glycerol, amylose and glycerol, as well as PLA and amylose. In order to reduce time and computer capacity to a reasonable level, simplified computational model systems for linear PLA and amylose were introduced. A trimer structure of three L-lactic acid monomer units was created for the

former in which the terminal hydrogens of both OH groups were replaced by methyls in order to avoid the formation of hydrogen-bonded complexes by them during geometry optimization. The amylose model system was a single monomer unit, that is, a single α-D-glucose molecule, in which the (1,4) OH groups were replaced by methoxy groups for the same reason. **Fig. 8** shows the corresponding structures indicating hydrogen bond donors (in blue) and acceptors (in red) as well as the acronym for each site used for the identification of the various hydrogen-bonded complexes. All possible donor-acceptor pairs were considered.

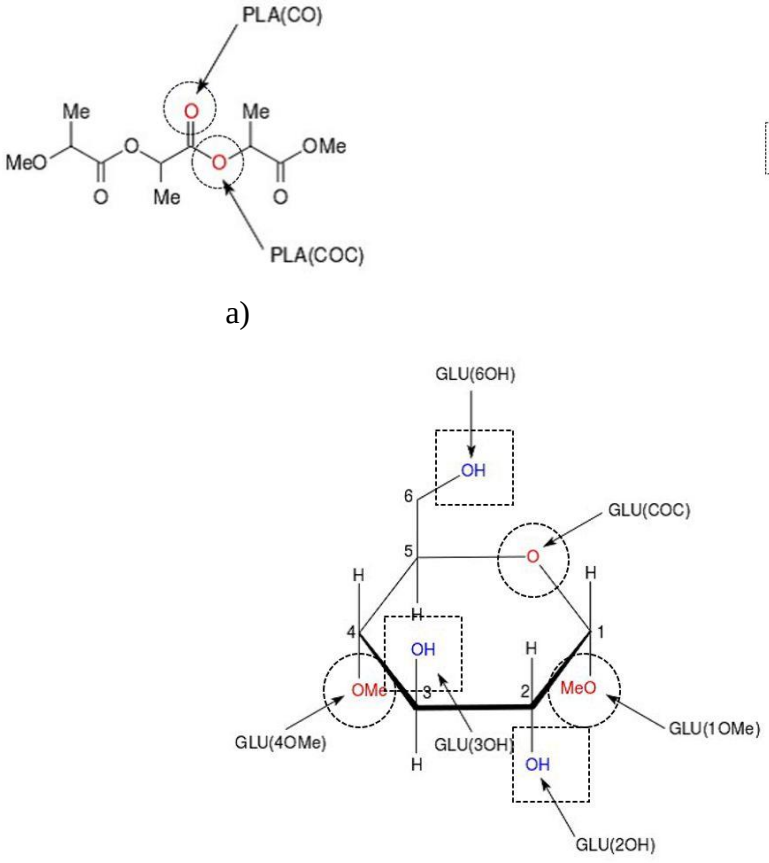

Fig. 8 Structure of the computational model systems and acronyms used for the identification of hydrogen bond donors (marked with square) and acceptors (marked with circle) studied in this work: (a) trimer of L-lactic acid with terminal methyl protection; (b) glycerol; (c) α-D-glucose with methyl protection on the (1,4)

OH groups.

Equilibrium structures for the individual donor and acceptor molecules were obtained separately from fully unconstrained optimizations using DFT with the M06-2X functional of Zhao and Truhlar [31], which accurately describes weak non-covalent interactions. For these calculations the 6-311++G** basis set [32] was used. The donors and acceptors were then linked into hydrogen bonded complexes, and unconstrained geometry optimizations were performed for these structures subsequently.

The total energies of the species were converted into enthalpies using the rotational constants and harmonic vibrational frequencies calculated at the reference geometries. Using the DFT equilibrium structures, additional single point energy calculations were also carried out at the LCCSD(T) [33] level with the aug-cc-pVTZ basis set [34, 35], where diffuse functions on hydrogen atoms were excluded. LCCSD(T) energies were also converted to enthalpies using corrections obtained from DFT calculations. Particularly, the difference between enthalpy and energy calculated with DFT was added to the energy obtained with LCCSD(T). Finally, the enthalpy of the hydrogen bonding interaction at both levels of theory was derived as the enthalpy difference between the complex and its constituent donor and acceptor sites. The Gaussian suite of programs [36] were invoked for the DFT calculations; all LCCSD(T) calculations were performed with MRCC [37].

Table 1 lists the calculated hydrogen bonding energies and enthalpies for the various donor-acceptor pairs defined by linking the corresponding model systems to each other. **Figs. 9a-c** show the three hydrogen bonded complexes with the smallest interaction enthalpies, that is, those structures of the three interacting pairs in which the strongest

hydrogen bonds form.

Table 1 Hydrogen bonding interaction energies and enthalpies calculated with the DFT and LCCSD(T) methods

Species	*M06-2X/6-311++G***		*LCCSD(T)/aug-cc-pVTZ*	
	ΔE (kJ/mol)	**ΔH** (kJ/mol)	**ΔE** (kJ/mol)	**ΔH** (kJ/mol)
GLY(1H)-PLA(CO)	-66	-56	-59	-49
GLY(2H)-PLA(CO)	-78	-68	-69	-59
GLY(1H)-PLA(COC)	-78	-67	-71	-60
GLY(2H)-PLA(COC)	-79	*-68*	-75	*-64*
GLY(1H)-GLU(1OMe)	-61	-52	-55	-46
GLY(2H)-GLU(1OMe)	-82	-71	-72	-61
GLY(1H)-GLU(2OH)	-87	-75	-77	-65
GLY(2H)-GLU(2OH)	-91	**-79**	-82	**-70**
GLY(1H)-GLU(3OH)	-76	-64	-66	-55
GLY(2H)-GLU(3OH)	-77	-65	-71	-59
GLY(1H)-GLU(4OMe)	-88	-76	-75	-63
GLY(2H)-GLU(4OMe)	-58	-48	-53	-43
GLY(1H)-GLU(6OH)	-75	-65	-69	-58
GLY(2H)-GLU(6OH)	-56	-46	-51	-41
GLY(1H)-GLU(COC)	-56	-46	-51	-41
GLY(2H)-GLU(COC)	-83	-72	-72	-61
PLA(CO)-GLU(2OH)	-65	-58	-60	-53
PLA(CO)-GLU(3OH)	-56	-50	-53	-47
PLA(CO)-GLU(6OH)	-52	-45	-52	-44
PLA(COC)-GLU(2OH)	-58	-52	-54	-47
PLA(COC)-GLU(3OH)	-50	-43	-45	-38
PLA(COC)-GLU(6OH)	-47	-42	-45	-39

According to our results presented in **Table 1**, the strongest interaction develops between glycerol and the model system of glucose. The hydrogen bonding enthalpies calculated with DFT and LCCSD(T) are -79 and -70 kJ/mol, respectively, and, as it can be

seen in **Fig. 9b**, three hydrogen bonds can form, in which both glucose and glycerol can act as donor and also acceptor at the same time. The interaction between glycerol and our PLA model is considerably weaker, binding enthalpies of -68 and -64 kJ/mol were obtained with DFT and LCCSD(T), respectively. In this case (**Fig. 9a**), two hydrogen bonds may form between the model PLA and glycerol. As shown in **Fig. 9c**, the formation of only a single hydrogen bond is possible between amylose and the polylactid acid model with a bonding enthalpy of -58 kJ/mol and -53 kJ/mol, respectively.

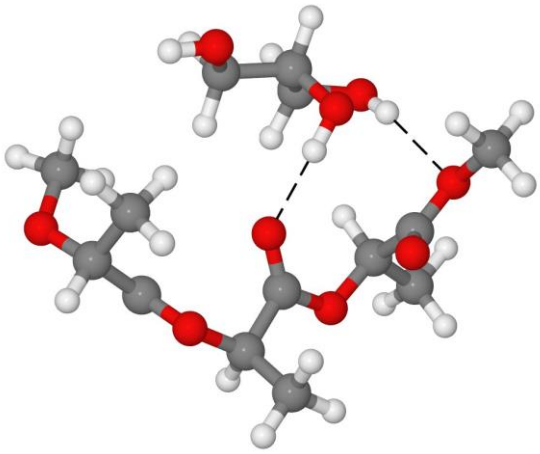

a)

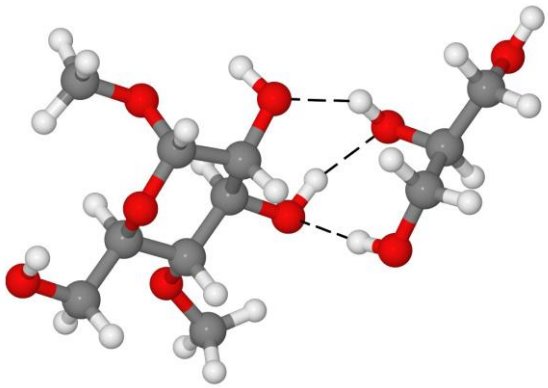

b)

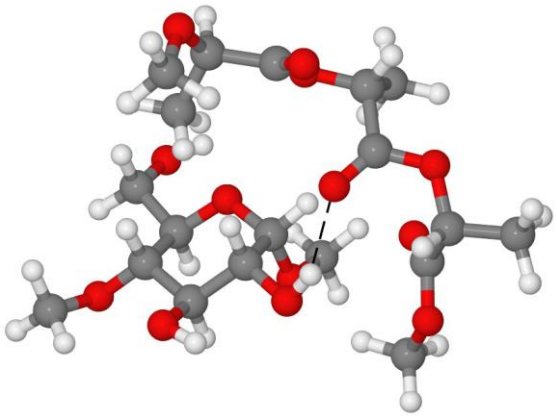

c)

Fig. 9 Formation of hydrogen bonds between various pairs of the components in the ternary system PLA/glycerol/starch; a) glycerol/lactic acid trimer, b) glycerol/glucose, c) lactic acid trimer/glucose

In order to estimate the amount of glycerol dissolving in PLA and starch, let us assume that the number of binding sites in both phases is significantly larger than the number of glycerol molecules available. Accordingly, the glycerol molecules can be attached to the site with the strongest binding enthalpy, i.e. using the notation of **Table 1**, the GLY(2H)-PLA(COC) and GLY(2H)-GLU(2OH) complexes can form in PLA and amylose, respectively. The ratio of concentrations can be approximated by the equilibrium constant of the GLY(2H)-PLA(COC) + GLU ⇌ PLA + GLY(2H)-GLU(2OH) reaction. If we assume that the binding entropy is approximately identical for the two complexes, the Gibbs free energy of the above reaction ($\Delta_r G$) equals the difference in the binding enthalpies of the complexes. Using the more accurate LCCSD(T) enthalpies, we obtain the value of $\Delta_r G$ = -6 kJ/mol from **Table 1**. Relying on the well-known formula for the equilibrium constant, $K = \exp(-\Delta_r G/RT)$, we arrive to K = 11 at room temperature indicating that the concentration of glycerol is at least by an order of magnitude larger in the amylose than in the PLA matrix.

Using the enthalpies determined in these calculations a lattice model was also created for the estimation of the mutual solubility of the polymer phases and the effect of glycerol on it. Either one glucose, one glycerol or three lactide units were placed in the cells of the lattice, respecrtively. The phase diagram was constructed from the change of free energy

$$\Delta G = \Delta H - T\Delta S \qquad (1)$$

where ΔG, ΔH and ΔS are the changes in the free energy, enthalpy and entropy of mixing. The change of entropy was calculated from the lattice model

$$\Delta S = \sum_{i=1}^{3} \frac{\varphi_i}{N_{p,i}} \ln \varphi_i \qquad (2)$$

where φ_i is the volume fraction of the components and $N_{p,i}$ their degree of polymerization. The change in enthalpy was calculated form the Flory-Huggins interaction parameter of the various pairs in the following way

$$\chi_{ij} = \frac{\varepsilon_{ij} - \frac{1}{2}(\varepsilon_{ii} - \varepsilon_{jj})}{RT} \qquad (3)$$

where ε_{ij} is the interaction enthalpy of the components, while ε_{ii} and ε_{jj} are the bonding enthalpy of like components at 298 K. Accordingly, the enthalpy of mixing is calculated from Eq. 4

$$\Delta H = RT(\chi_{12}\varphi_1\varphi_2 + \chi_{13}\varphi_1\varphi_3 + \chi_{23}\varphi_2\varphi_3) \qquad (4)$$

where R is the universal gas constant and T the absolute temperature. The calculated phase diagram is shown in **Fig. 10**. Dashed black lines connect the compositions of phases, which are in equilibrium at various glycerol contents of TPS. The results of the calculations and **Fig. 10** clearly show that most of the glycerol is located in the starch phase. Blue points and lines show the compositions of the TPS/PLA blends studied in this work. Neat PLA and neat TPS are the endpoints of the blue lines while the composition of the blends are

located between these two extremes. All compositions studied are located in the two phase range of the diagram, i.e. they phase separate to PLA and starch containing small amount of PLA.

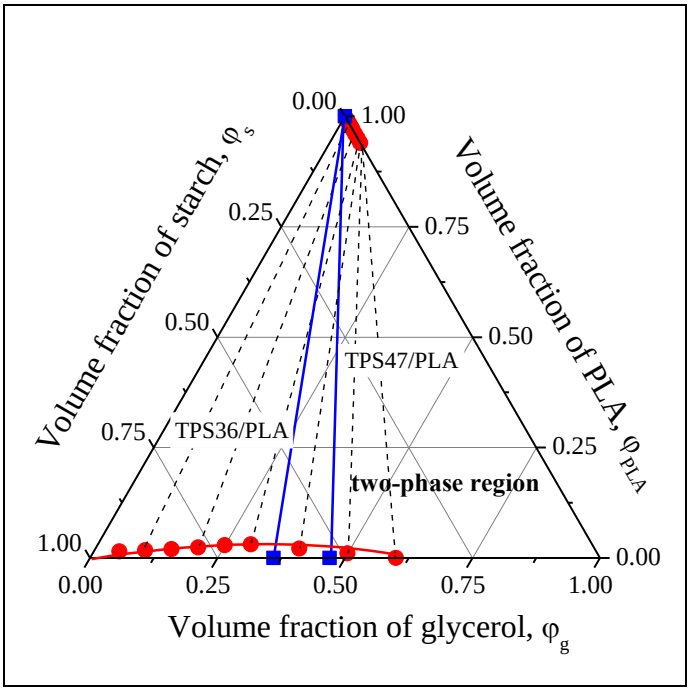

Fig. 10 Calculated phase diagram of the ternary system PLA/starch/glycerol; effect of glycerol on miscibility.

The phase diagram unambiguously shows that PLA does not dissolve any TPS at all, while it can be dissolved in a small extent, about 3 vol % at most, in plasticized starch. Glycerol facilitates the dissolution of PLA in TPS, a conclusion which is in agreement with those of Ma et al. [9, 10] who found that a plasticizer can improve the compatibility of PLA and TPS. On the other hand, these calculations also confirm that the majority of glycerol molecules is located in the TPS phase and do not diffuse into PLA. We must emphasize here, though, that these calculations are very qualitative in manner giving information only about the direction and magnitude of changes brought about by the mixing the two components.

3.4. Structure

The phase structure of the PLA/TPS blends was studied by scanning electron microscopy. Etched surfaces were prepared in order to help the clear distinction of the phases. Three micrographs are presented in **Fig. 11** to demonstrate the effect of composition on structure.

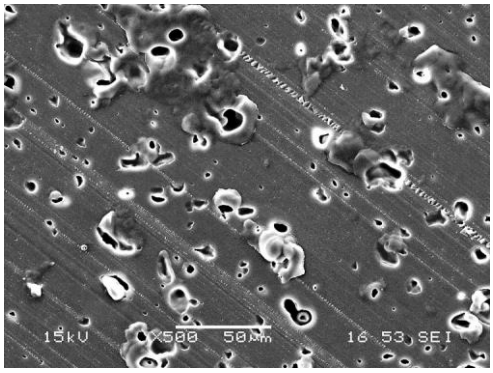

a)

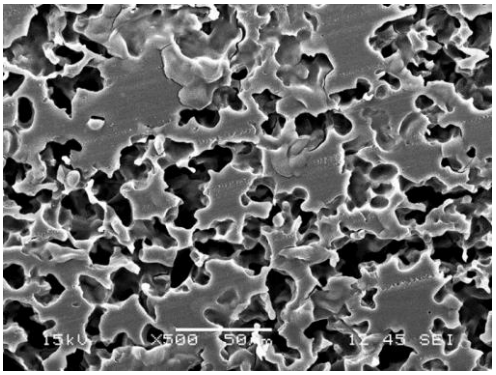

b)

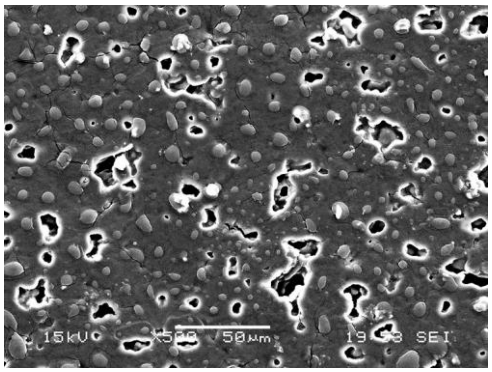

c)

Fig. 11 Effect of composition on the dispersed structure of PLA/TPS blends, SEM

micrographs at magnification 500x; a) 10, b) 50, c) 90 vol% TPS.

In accordance with previous results, heterogeneous structure forms at all compositions. PLA is the continuous phase at large PLA and small TPS content in which TPS is dispersed in the form of droplets of a few micron size (**Fig. 11a**). The opposite occurs at the other end of the composition range, PLA is dispersed as small particles in the continuous TPS phase here (**Fig. 11c**). A more or less co-continuous structure develops at around 50 vol% of both components as shown by **Fig. 11b**. The concentration range of co-continuous structure is very narrow, dispersed structure was observed at both sides of 50/50 composition, i.e. at 40 and 60 vol% TPS content. Both the dispersed structure and the narrow range of the interpenetrating network like structure are in strong agreement with the rest of our conclusions about the immiscibility of the two components and the development of only weak interactions between the phases.

3.5. Properties

Conclusions about compatibility are often drawn from the composition dependence of mechanical properties. However, the characteristics of the components differ considerably from each other in our case, composition dependence is dominated by this difference and it is very difficult to arrive to any reasonable conclusion as a consequence. This statement is demonstrated adequately by **Fig. 12** showing the composition dependence of the Young's modulus for the two sets of blends. The stiffness of PLA is approximately 3 GPa, while it is around 60 MPa and less than 1 MPa for TPS36 and TPS47, respectively. Young's modulus decreases quite rapidly with increasing TPS content and the stiffness of the blends is always smaller than the one predicted by additivity, indicating again weak interactions.

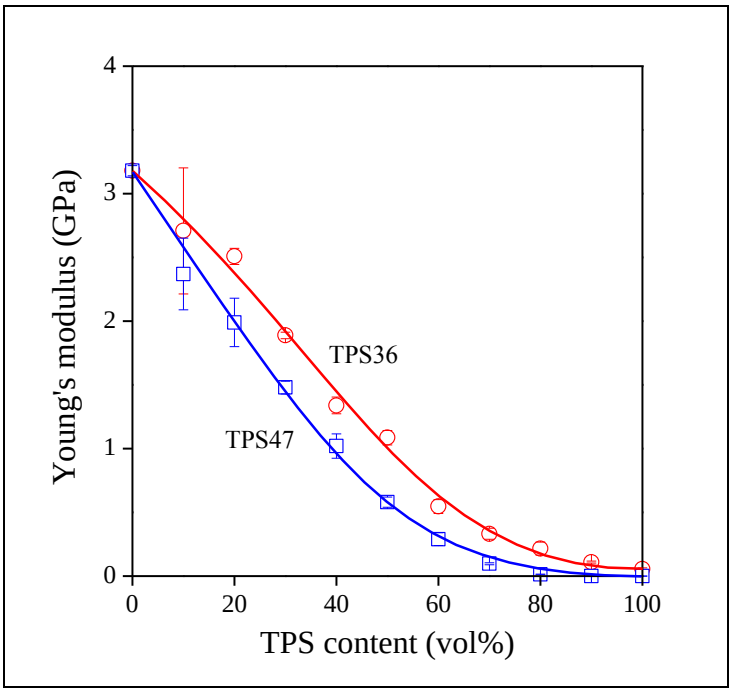

Fig. 12 Composition dependence of the Young's modulus of PLA/TPS blends; (○) TPS36, (□) TPS47.

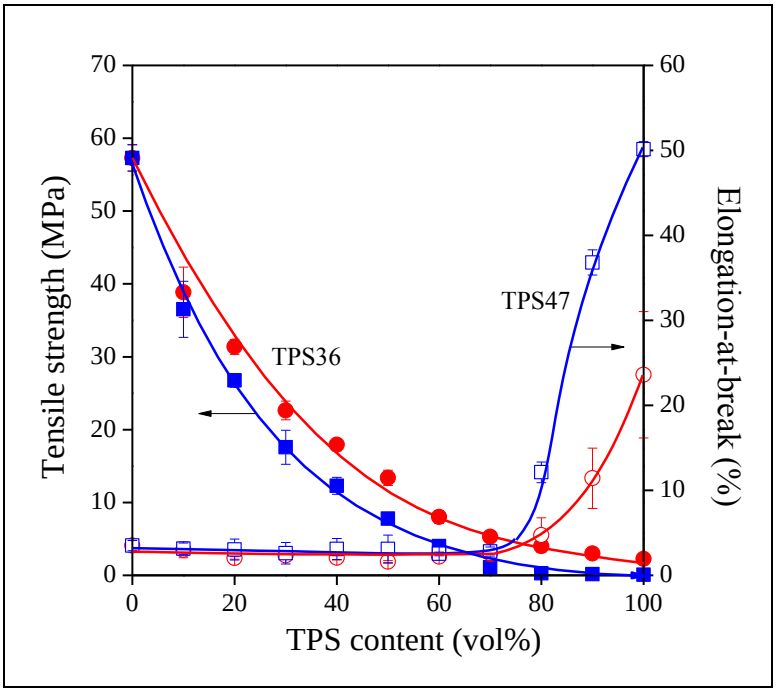

Fig. 13 Tensile strength and elongation-at-break of PLA/TPS blends plotted against TPS content; (○,●) TPS36, (□,■) TPS47; full: strength, empty: elongation-at-break.

The composition dependence of mechanical characteristics measured at yielding and at break is very similar to each other. Tensile strength and elongation-at-break are plotted against TPS content in **Fig. 13**. The correlations offer limited information again. The strength of PLA deteriorates rapidly with increasing TPS content almost independently of glycerol content. The negative deviation from additivity indicates strong incompatibility of the components. The deformability of PLA and most of the blends is very small forecasting also poor impact properties that was confirmed by independent measurements. Changes in the elongation-at-break values of the blends shows that TPS properties dominate above 80 vol% TPS content, but PLA decreases the deformability of TPS quite fast. Obviously the properties of these PLA/TPS blends are moderate at most and some coupling strategy much be applied in order to develop a material for practical use.

4. Conclusions

A detailed analysis of experimental results obtained on PLA/TPS blends supported by model calculations showed that the interaction of the two components is weak. The investigation of the possible partitioning of glycerol in the two phases indicated that most of the plasticizer is located in the TPS phase and does not diffuse into PLA. Thermodynamic modeling predicted some dissolution of PLA in TPS which was assisted by the presence of the plasticizer, but TPS does not dissolve in PLA at all. As a consequence of weak interactions, properties are moderate at most. Blending of the two components resulted in heterogeneous, two phase structure at all compositions. No tangible proof was found for the formation of a glycerol rich phase in TPS, the relaxation transition assigned to this phase was rather explained with the movement of smaller structural units

of starch molecules. Weak interfacial adhesion does not allow stress transfer through the interface resulting in poor strength and small deformation. TPS deteriorates the properties of PLA considerably, but blends with a starch matrix are also extremely weak. Useful materials can be produced from PLA and TPS only with the development of an appropriate coupling strategy.

5. Acknowledgements

The authors acknowledge the support of the National Scientific Research Fund of Hungary (OTKA Grant No. K 120039 and 108934) for this project on interactions and structure-property correlations in polymer blends. The research work has been part of the BME R+D+I project supported by the TÁMOP grant No. 4.2.1/B-09/1/KMR-2010-0002. The authors acknowledge the computing time granted on the Hungarian HPC Infrastructure at NIIF Institute, Hungary.

6. References

1. Chakraborty A, Sain M, Kortschot M, and Cutler S. Dispersion of wood microfibers in a matrix of thermoplastic starch and starch-polylactic acid blend. Journal of Biobased Materials and Bioenergy 2007;1(1):71-77.
2. Shirai MA, Grossmann MVE, Mali S, Yamashita F, Garcia PS, and Müller CMO. Development of biodegradable flexible films of starch and poly(lactic acid) plasticized with adipate or citrate esters. Carbohydrate Polymers 2013;92(1):19-22.
3. Teixeira ED, Curvelo AAS, Correa AC, Marconcini JM, Glenn GM, and Mattoso LHC. Properties of thermoplastic starch from cassava bagasse and cassava starch

and their blends with poly (lactic acid). Industrial Crops and Products 2012;37(1):61-68.

4. Huneault MA and Li H. Morphology and properties of compatibilized polylactide/thermoplastic starch blends. Polymer 2007;48(1):270-280.
5. Li H and Huneault MA. Comparison of sorbitol and glycerol as plasticizers for thermoplastic starch in TPS/PLA blends. Journal of Applied Polymer Science 2011;119(4):2439-2448.
6. Avérous L, Moro L, Dole P, and Fringant C. Properties of thermoplastic blends: starch–polycaprolactone. Polymer 2000;41(11):4157-4167.
7. Avérous L and Fringant C. Association between plasticized starch and polyesters: Processing and performances of injected biodegradable systems. Polymer Engineering & Science 2001;41(5):727-734.
8. Martin O and Avérous L. Poly(lactic acid): plasticization and properties of biodegradable multiphase systems. Polymer 2001;42(14):6209-6219.
9. Wang N, Yu J, Chang PR, and Ma X. Influence of formamide and water on the properties of thermoplastic starch/poly(lactic acid) blends. Carbohydrate Polymers 2008;71(1):109-118.
10. Wang N, Yu J, and Ma X. Preparation and characterization of compatible thermoplastic dry starch/poly(lactic acid). Polymer Composites 2008;29(5):551-559.
11. Zhang K, Mohanty AK, and Misra M. Fully biodegradable and biorenewable ternary blends from polylactide, poly(3-hydroxybutyrate-co-hydroxyvalerate) and poly(butylene succinate) with balanced properties. Acs Applied Materials & Interfaces 2012;4(6):3091-3101.
12. Yokesahachart C and Yoksan R. Effect of amphiphilic molecules on characteristics

and tensile properties of thermoplastic starch and its blends with poly(lactic acid). Carbohydrate Polymers 2011;83(1):22-31.

13. Ren J, Fu H, Ren T, and Yuan W. Preparation, characterization and properties of binary and ternary blends with thermoplastic starch, poly(lactic acid) and poly(butylene adipate-co-terephthalate). Carbohydrate Polymers 2009;77(3):576-582.

14. Kalichevsky MT, Jaroszkiewicz EM, and Blanshard JMV. A study of the glass transition of amylopectin—sugar mixtures. Polymer 1993;34(2):346-358.

15. Forssell PM, Mikkilä JM, Moates GK, and Parker R. Phase and glass transition behaviour of concentrated barley starch-glycerol-water mixtures, a model for thermoplastic starch. Carbohydrate Polymers 1997;34(4):275-282.

16. Lourdin D, Coignard L, Bizot H, and Colonna P. Influence of equilibrium relative humidity and plasticizer concentration on the water content and glass transition of starch materials. Polymer 1997;38(21):5401-5406.

17. Mikus PY, Alix S, Soulestin J, Lacrampe MF, Krawczak P, Coqueret X, and Dole P. Deformation mechanisms of plasticized starch materials. Carbohydrate Polymers 2014;114:450-457.

18. Kalogeras IM. Glass-transition phenomena in polymer blends. Encyclopedia of Polymer Blends: Wiley-VCH Verlag GmbH & Co. KGaA, 2016. pp. 1-134.

19. Dudowicz J, Douglas JF, and Freed KF. Two glass transitions in miscible polymer blends? The Journal of Chemical Physics 2014;140(24):244905.

20. Shi P, Schach R, Munch E, Montes H, and Lequeux F. Glasst transition distribution in miscible polymer blends: from calorimetry to rheology. Macromolecules 2013;46(9):3611-3620.

21. Számel G, Klébert S, Sajó I, and Pukánszky B. Thermal analysis of cellulose

acetate modified with caprolactone. Journal of Thermal Analysis and Calorimetry 2008;91(3):715-722.

22. Dominkovics Z, Dányádi L, and Pukánszky B. Surface modification of wood flour and its effect on the properties of PP/wood composites. Composites Part a-Applied Science and Manufacturing 2007;38(8):1893-1901.

23. Stading M, Rindlav-Westling Å, and Gatenholm P. Humidity-induced structural transitions in amylose and amylopectin films. Carbohydrate Polymers 2001;45(3):209-217.

24. Müller P, Imre B, Bere J, Móczó J, and Pukánszky B. Physical ageing and molecular mobility in PLA blends and composites. Journal of Thermal Analysis and Calorimetry 2015;122(3):1423-1433.

25. Molnár K, Móczó J, Murariu M, Dubois P, and Pukánszky B. Factors affecting the properties of PLA/$CaSO_4$ composites: homogeneity and interactions. Express Polymer Letters 2009;3(1):49-61.

26. Booij HC. Effect of thermal stresses on the dynamic moduli of ABS-resins. British Polymer Journal 1977;9(1):47-55.

27. Kolárik J, Lednicky F, Jancár J, and Pukánszky B. Phase structure of ternary composites consisting of polypropylene/elastomer/filler. Effect of functionalized components. Polymer Communications 1990;31(5):201-204.

28. Mäder D, Bruch M, Maier R-D, Stricker F, and Mülhaupt R. Glass transition temperature depression of elastomers blended with poly(propene)s of different stereoregularities. Macromolecules 1999;32(4):1252-1259.

29. Szabó P, Epacher E, Földes E, and Pukánszky B. Miscibility, structure and properties of PP/PIB blends. Materials Science and Engineering A 2004;383(2):307-315.

30. Thirtha V, Lehman R, and Nosker T. Morphological effects on glass transition behavior in selected immiscible blends of amorphous and semicrystalline polymers. Polymer 2006;47(15):5392-5401.

31. Zhao Y and Truhlar D. The M06 suite of density functionals for main group thermochemistry, thermochemical kinetics, noncovalent interactions, excited states, and transition elements: two new functionals and systematic testing of four M06-class functionals and 12 other functionals. Theoretical Chemistry Accounts 2008;120(1-3):215-241.

32. Krishnan R, Binkley JS, Seeger R, and Pople JA. Self-consistent molecular orbital methods. XX. A basis set for correlated wave functions. The Journal of Chemical Physics 1980;72(1):650-654.

33. Rolik Z, Szegedy L, Ladjánszki I, Ladóczki B, and Kállay M. An efficient linear-scaling CCSD(T) method based on local natural orbitals. The Journal of Chemical Physics 2013;139(9):094105.

34. Kendall RA, Dunning TH, and Harrison RJ. Electron affinities of the first-row atoms revisited. Systematic basis sets and wave functions. The Journal of Chemical Physics 1992;96(9):6796-6806.

35. Dunning TH. Gaussian basis sets for use in correlated molecular calculations. I. The atoms boron through neon and hydrogen. The Journal of Chemical Physics 1989;90(2):1007-1023.

36. Frisch MJ, Trucks GW, Schlegel HB, Scuseria GE, Robb MA, Cheeseman JR, Scalmani G, Barone V, Mennucci B, Petersson GA, Nakatsuji H, Caricato M, Li X, Hratchian HP, Izmaylov AF, Bloino J, Zheng G, Sonnenberg JL, Hada M, Ehara M, Toyota K, Fukuda R, Hasegawa J, Ishida M, Nakajima T, Honda Y, Kitao O, Nakai H, Vreven T, Montgomery Jr. JA, Peralta JE, Ogliaro F, Bearpark MJ, Heyd

J, Brothers EN, Kudin KN, Staroverov VN, Kobayashi R, Normand J, Raghavachari K, Rendell AP, Burant JC, Iyengar SS, Tomasi J, Cossi M, Rega N, Millam NJ, Klene M, Knox JE, Cross JB, Bakken V, Adamo C, Jaramillo J, Gomperts R, Stratmann RE, Yazyev O, Austin AJ, Cammi R, Pomelli C, Ochterski JW, Martin RL, Morokuma K, Zakrzewski VG, Voth GA, Salvador P, Dannenberg JJ, Dapprich S, Daniels AD, Farkas Ö, Foresman JB, Ortiz JV, Cioslowski J, and Fox DJ. Gaussian 09. Wallingford, CT, USA: Gaussian, Inc., 2009.

37. Kállay M, Rolik Z, Ladjánszki I, Szegedy L, Ladóczki B, Csontos J, and Kornis B. MRCC. MRCC, a quantum chemical program suite See also ref [33] as well as www.mrcc.hu.

TOC